AAAS
Research
Volume 2022, Article ID 9784309, 12 pages
https://doi.org/10.34133/2022/9784309

Research Article

Room-Temperature Superconductivity in Yb/Lu Substituted Clathrate Hexahydrides under Moderate Pressure

Mingyang Du,[1] Hao Song,[1] Zihan Zhang,[1] Defang Duan,[1] and Tian Cui[1,2]

[1]*College of Physics, Jilin University, Changchun 130012, China*
[2]*Institute of High-Pressure Physics, School of Physical Science and Technology, Ningbo University, Ningbo 315211, China*

Correspondence should be addressed to Defang Duan; duandf@jlu.edu.cn and Tian Cui; cuitian@nbu.edu.cn

Received 9 May 2022; Accepted 18 July 2022; Published 9 August 2022

Room temperature superconductivity is a dream that mankind has been chasing for a century. In recent years, the synthesis of H_3S, LaH_{10}, and C-S-H compounds under high pressures has gradually made that dream become a reality. But the extreme high pressure required for stabilization of hydrogen-based superconductors limit their applications. So, the next challenge is to achieve room-temperature superconductivity at significantly low pressures, even ambient pressure. In this work, we design a series of high temperature superconductors that can be stable at moderate pressures by incorporating heavy rare earth elements Yb/Lu into sodalite-like clathrate hexahydrides. In particular, the critical temperatures (T_c) of Y_3LuH_{24}, $YLuH_{12}$, and YLu_3H_{24} can reach 283 K at 120 GPa, 275 K at 140 GPa, and 288 K at 110 GPa, respectively. Their critical temperatures are close to or have reached room temperature, and minimum stable pressures are significantly lower than that of reported room temperature superconductors. Our work provides an effective method for the rational design of low-pressure stabilized hydrogen-based superconductors with room-temperature superconductivity simultaneously and will stimulate further experimental exploration.

1. Introduction

Since H. K. Onnes observed the superconductivity of Hg in 1911, researchers have been trying many ways to find new superconductors or improve their superconducting properties. For example, cuprate high-temperature superconductor $HgBa_2Ca_2Cu_3O_{8+\delta}$ with critical temperature (T_c) of 133 K was discovered [1], whose T_c was improved to 164 K in diamond anvil cells [2]; the T_c of $Bi_2Sr_2CaCu_2O_{8+\delta}$ was altered from 84 K to 94 K via a shockwave treatment [3]. Recently, many hydrides with T_cs exceeding 200 K were discovered under high pressure [4–6], e.g., H_3S with 203 K at 155 GPa [7–10] and LaH_{10} with 250-160 K at 170 GPa [11–14].

Among these hydrogen-based superconductors, clathrate hydrides are one type that exists widely, including the well-known CaH_6 with H_{24} cage [15], YH_9 with H_{29} cage [16], and LaH_{10} with H_{32} cage [11, 12]. The clathrate hexahydrides *Im*-3m-XH_6 (X = Mg, Ca, Sc, Y, La, Tm, Yb, and Lu) are prevalent in alkaline earth and rare earth metal hydride [12, 15, 17–20], in which, the metal atoms form a body centered cubic (bcc) lattice, and hydrogen atoms occupy all the tetrahedral voids of the bcc lattice, forming a H_{24} cage. CaH_6 and YH_6 have been experimentally synthesized and exhibit high T_c of 215 K at 172 GPa and 227 K at 166 GPa, respectively [21, 22]. Theoretical predicted T_cs of MgH_6, ScH_6, and LaH_6 are 260 K at 300 GPa, 147 K at 285 GPa, and 174 K at 100 GPa, respectively. It is reported that the large chemical precompression of H-rich clathrate structures can be attained in rare earth hydrides with 4*f* electrons [23]. With the filling of the *f* orbitals of metal atoms, the structure is more easily stabilized at low pressure, but the unfilled *f* electrons can negatively affect superconductivity. For example, the CeH_9 with unfilled 4*f* orbitals were experimentally synthesized at low pressure of 88 GPa with low T_c of 57 K [24]. TmH_6, with unfilled 4*f* orbitals, is predicted to stable at 50 GPa and has a lower T_c of 25 K. YbH_6 and LuH_6, with filled *f*-shelled, are predicted to exhibit high-T_c superconductivity of 145 K and 273 K at relatively low pressures of 70 GPa and 100 GPa, respectively [20]. These results suggest that heavy rare earth metals Yb/

Lu are suitable elements to reduce the pressure of stability and keep high T_c simultaneously.

Incorporating a new element into binary hydrides to form ternary hydrides is an important way to improve the superconducting transition temperature or reduce the superconducting phase stable pressure. In 2019, Li_2MgH_{16} with the highest T_c to date (473 K at 250 GPa) was designed by introducing extra electrons (Li element) to fill the antibonding orbital of the H_2 molecular units of MgH_{16} [25]. In 2020, a compound of hydrogen, carbon, and sulfur showed a superconducting transition at 288 K [26] and 267 GPa. However, the stoichiometry and crystal structure of this compound have not yet been determined. This experiment is still subject to many controversies [16, 27, 28]. Although the T_cs of Li_2MgH_{16} and C-S-H compounds can reach room temperature, the extreme pressure above 250 GPa also makes them difficult in practical application. Recently, a new class of fluorite-type clathrate ternary hydrides AXH_8 (A = Ca, Sr, Y, and La, X = B, Be, and Al) with hydrogen alloy backbone were predicted [29]. The most outstanding one, $LaBeH_8$, is dynamically stable down to 20 GPa with a high T_c ~185 K. It is inspiring that the cubic clathrate superhydrides $La_xY_{1-x}H_{6,10}$ via laser heating of yttrium–lanthanum alloys have been experimental synthesized exhibiting a maximum critical temperature T_c of 253 K without increasing pressure [30]. This experiment demonstrates that selecting a suitable central metal element to substitute sodalite-like clathrate hydrides is feasible.

The focus of hydrogen-based superconductor research is not simply the pursuit of high-temperature superconductivity or low stable pressure. A good superconductor should achieve a good balance between the pressure required for stability and the critical temperature. The next challenge is to achieve room-temperature superconductivity at significantly low pressures, even ambient pressure. In the present work, we chose heavy rare earth element Yb/Lu-doped clathrate hexahydrides to achieve this goal. According to the aforementioned introduction, the heavy rare earth metals Yb/Lu show outstanding properties in sodalite-like clathrate hexahydrides YbH_6 and LuH_6. With full-filled f-shells, Yb/Lu can eliminate the negative impact on T_c of f electrons, meanwhile satisfying the purpose of reducing the pressure.

Here, a serial of ternary hydrides $A_{1-x}B_xH_6$ (A = Y, Ca, Sc, B=Yb, Lu, and A = Yb, B = Lu, x = 0.25, 0.33, 0.5, 0.67, 0.75) with high T_c at moderate pressure were found, in which the atomic radii of A and B are similar. Among them, the critical temperatures of Y_3LuH_{24}, $YLuH_{12}$, and YLu_3H_{24} are 283 K at 120 GPa, 275 K at 140 GPa, and 288 K at 110 GPa, respectively, which are close to or have reached room temperature. Recently, it is reported that pressure-induced high-temperature superconducting FeSe retained without pressure via pressure quenching (PQ) [31]. This PQ technique offers the possibility of these high T_c hydrides for practical application in the future.

2. Results

We first performed an extensive variable composition structure searches of ternary hydrides Y-Lu-H, Ca-Lu-H, and Yb-Lu-H under high pressure. Six sodalite-like clathrate structures $A_{1-x}B_xH_6$ (A = Y, Ca, and Yb, B = Lu, x = 0.25, 0.33, 0.5, 0.67, 0.75) were found in our structure searches, including Pm-3m and Fd-3m of ABH_{12}, P-3m1-AB_2H_{18}, P-3m1-A_2BH_{18}, Fm-3m-AB_3H_{24}, and Fm-3m-A_3BH_{24} (see Figure 1). The thermodynamic stability of these structures was determined by constructing convex hulls (see Figures S1–S4). YLu_3H_{24}, $YLuH_{12}$, Y_3LuH_{24}, $CaLuH_{12}$, $CaLu_3H_{24}$, and Yb_2LuH_{18} are thermodynamically stable at 300 GPa, and Ca_3LuH_{24} can be thermodynamically stable at 200 GPa. In addition to hexahydrides, several thermodynamically stable ternary hydrides such as $YLuH_8$, Y_3LuH_{20}, $CaLu_3H_3$, and Ca_3LuH_{15} were discovered, which will not be discussed in depth in this work (see Figures S1–S4).

In order to extend the study to more ternary hydride systems, we substitute the metal elements in these six structures. The properties of clathrate structure can be further improved by choosing a suitable "precompressor" element. As discussed above, at least one of them is heavy rare earth element Yb/Lu, and the other element has similar radius with Yb/Lu, including K, Mg, Ca, Sr, Sc, Y, and La. We calculated the phonon dispersion for all possible components in the pressure range of 50-200 GPa and finally determined that 36 sodalite-like clathrate hexahydrides can be dynamically stable in seven ternary hydride systems, including Y-Lu-H, Ca-Lu-H, Sc-Lu-H, Y-Yb-H, Ca-Yb-H, Sc-Yb-H, and Yb-Lu-H (see Figures S9–S15). To determine the thermodynamic stability of these structures in Y-Yb-H, Ca-Yb-H, Sc-Lu-H, and Sc-Yb-H system, we also performed the fixed composition structure searches of $A_xB_{1-x}H_6$ and constructed the convex hull, shown in Figures S5–S8. It is reported that the YH_6, CaH_6, and YbH_6 are always thermodynamically stable in the pressure range of 150–300 GPa. Therefore, the energetic stabilities of the Yb-containing hexahydrides in Y-Yb-H and Ca-Yb-H system are evaluated using their formation enthalpies (ΔH) with respect to binary hexahydrides. Compared with Lu-containing hexahydrides, many Yb-containing hexahydrides can be thermodynamically stable at 200 GPa, including $CaYbH_{12}$, Ca_3YbH_{24}, $CaYb_3H_{24}$, and $YYbH_{12}$. All Sc-containing sodalite-like clathrate hexahydrides we studied are metastable phases in our studied pressure range (see Figures S7 and S8).

After determining the stability of all structures, we further calculated their superconducting properties. The superconductive transition temperatures of these structures are estimated through the Allen–Dynes-modified McMillan equation with correction factors and self-consistent solution of the Eliashberg equation (see Table S1). We also calculated the critical temperatures of CaH_6 and YH_6 in the same way and compared them with the experimentally measured values (see Table S2). The results show that the critical temperature T_c using the self-consistent solution of the Eliashberg equation is in good agreement with the experimental measurements.

Figure 2 shows the variation of critical temperature T_c and minimum dynamically stable pressure with the concentration of heavy rare earth element Lu/Yb in sodalite-like clathrate hexahydrides. YH_6 has more excellent properties

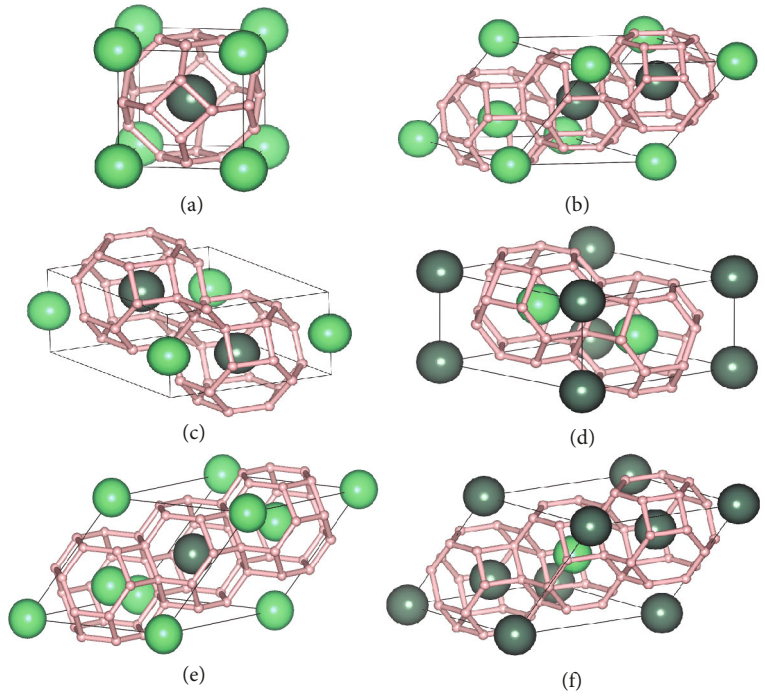

FIGURE 1: Crystal structures of (a) *Pm*-3m-$ABLuH_{12}$, (b) *Fd*-3*m*-ABH_{12}, (c) *P*-3*m*1-AB_2H_{18}, (d) *P*-3*m*1-A_2BH_{18}, (e) *Fm*-3*m*-AB_3H_{24}, and (f) *Fm*-3*m*-A_3BH_{24}. The light green and dark green balls represent "precompressor" metal atoms A and B, respectively. The small pink balls represent H atoms.

than CaH_6 and ScH_6, and its properties are further improved after incorporation of Lu. The results show that YLu_2H_{18} and Y_2LuH_{18} with the *P*-3m1 space group have similar properties, with high T_c of 242 K and 240 K at 100 GPa, respectively (see Figure 2(a)). And YLu_3H_{24} and Y_3LuH_{24} with the *Fm*-3m space group also have very close properties, exhibiting room temperature of 288 K at 110 GPa and 283 K at 120 GPa, respectively. The critical temperature of $YLuH_{12}$ with space group *Pm*-3*m* is 275 K at 140 GPa, reaching ice point temperature. The critical temperatures of Y_3LuH_{24}, $YLuH_{12}$, and YLu_3H_{24} are close to or have reached room temperature. Surprisingly, the images of T_c and minimum pressure of $Y_{(1-x)}Lu_xH_6$ exhibit mirror symmetry as a function of Lu doping concentration due to their similar properties (see Figure 2(a)). For $Y_{(1-x)}Lu_xH_6$, the structure appears to have a greater effect on the T_c and minimum pressure than the doping concentration.

For CaH_6, both T_c and minimum pressure show a trend of first increasing and then decreasing with the Lu doping concentration (see Figure 2(b)). Ca_3LuH_{24} has a T_c of 221 K at 170 GPa, which is close to CaH_6. At 170 GPa, the critical temperature of $CaLuH_{12}$ is 282 K, near room temperature. And $CaLu_2H_{18}$ can be dynamically stable at 140 GPa, and its T_c is as high as 299 K at this pressure, which is the highest T_c in this work. It is only 6 meV/atom above the convex hull at 300 GPa, implying the possibility of experimental synthesis. For ScH_6, doping with Lu can significantly reduce the minimum stable pressure and increase T_c. With the increase of Lu doping concentration in $Sc_{(1-x)}Lu_xH_6$, T_c showed an upward trend, and the minimum pressure is basically maintained at about 100 GPa (see Figure 2(c)). The effect of Lu on reducing the minimum pressure is obvious. The most prominent is $ScLu_3H_{24}$, which reaches a T_c of 271 K at 100 GPa, close to ice point temperature. In short, doping Lu in binary hexahydrides achieves the goal of reducing the dynamical stable pressure and increasing T_c, such as $YLuH_{12}$ (275 K at 140 GPa), YLu_3H_{24} (288 K at 110 GPa), Y_3LuH_{24} (283 K at 120 GPa), $CaLuH_{12}$ (282 K at 170 GPa), and $CaLu_2H_{18}$ (299 K at 140 GPa).

The T_cs of Yb-containing structures are all significantly lower than those of Lu-containing structures and show a decreasing trend with the increase of doping concentration of Yb. There are only five low Yb concentration hydrides have T_c over 200 K, such as Y_3YbH_{24} (222 K at 100 GPa), Y_2YbH_{18} (221 K at 100 GPa), Sc_3YbH_{24} (203 K at 100 GPa), $YbLu_2H_{18}$ (212 K at 150 GPa), and $YbLu_3H_{24}$ (222 K at 100 GPa). The effect of Yb on reducing the dynamical stable pressure is obvious. The minimum dynamically stable pressure of $Y_{(1-x)}Yb_xH_6$ is basically maintained around 100 GPa (see Figure 2(d)). But for $Ca_{(1-x)}Yb_xH_6$, the introduction of heavy rare earth element cannot always reduce the dynamically stable pressure (see Figure 2(e)). The minimum dynamically stable pressure of $CaYbH_{12}$ and Ca_3YbH_{24} is 150 GPa like that of CaH_6, and the minimum dynamically stable pressure of Ca_2YbH_{18} is even higher than that of CaH_6, reaching 170 GPa. Only $CaYb_2H_{18}$ and $CaYb_3H_{24}$ with Yb concentrations over 50% exhibit lower pressures than CaH_6, with minimum dynamically stable pressures of 130 GPa and 100 GPa, respectively. This is similar to $Ca_{(1-x)}Lu_xH_6$ discussed above. Doping less than 50% Yb/Lu in CaH_6 cannot reduce the dynamically stable pressure. This is due to the large difference between the radius of Ca and Yb/Lu. The minimum

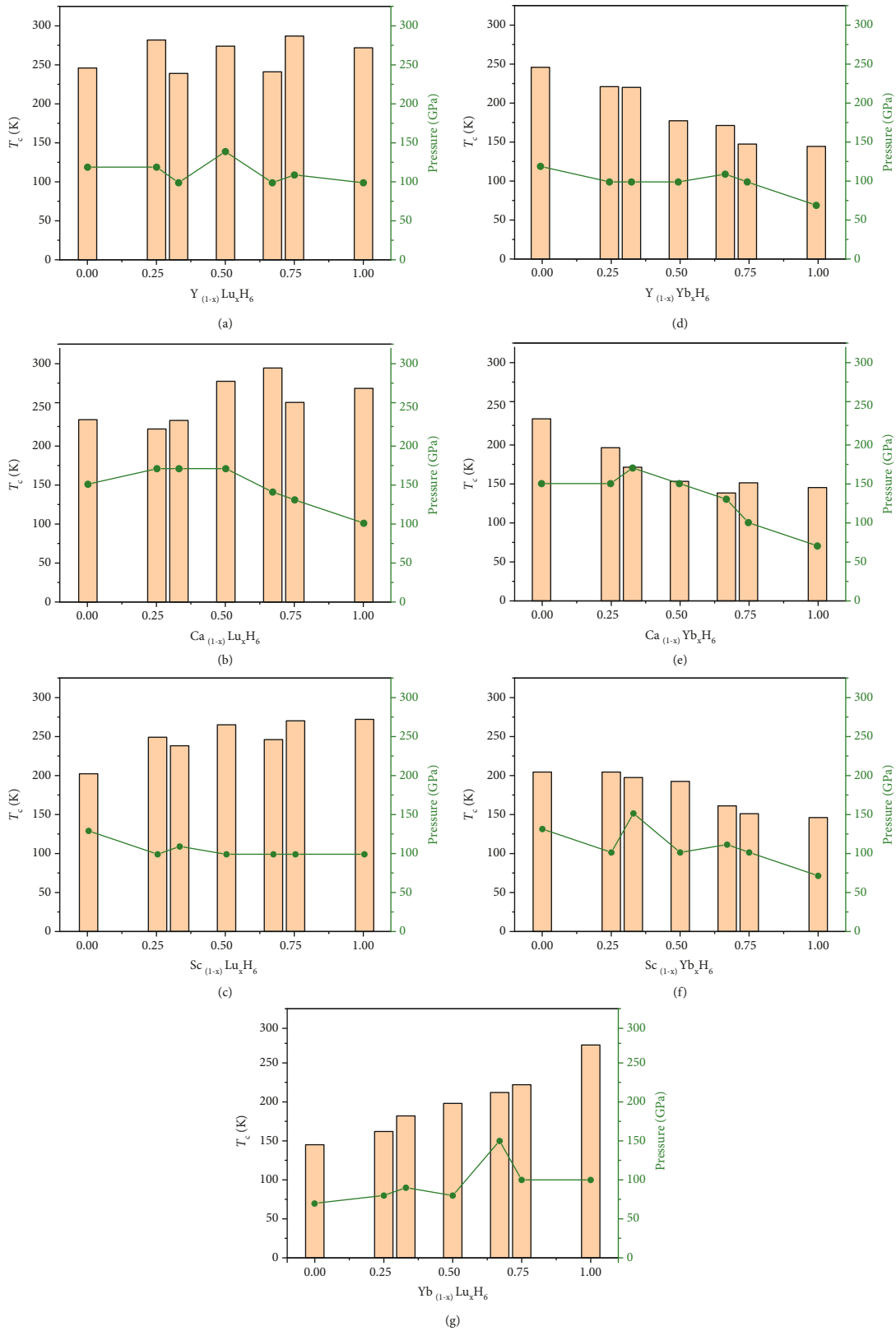

FIGURE 2: The calculated superconducting critical temperature T_c using the self-consistent solution of the Eliashberg equation and the minimum dynamically stable pressure as a function of doping concentration in (a) $Y_{(1-x)}Lu_xH_6$, (b) $Ca_{(1-x)}Lu_xH_6$, (c) $Sc_{(1-x)}Lu_xH_6$, (d) $Y_{(1-x)}Yb_xH_6$, (e) $Ca_{(1-x)}Yb_xH_6$, (f) $Sc_{(1-x)}Yb_xH_6$, and (g) $Yb_{(1-x)}Lu_xH_6$. The Coulomb pseudopotential is using $\mu^* = 0.13$.

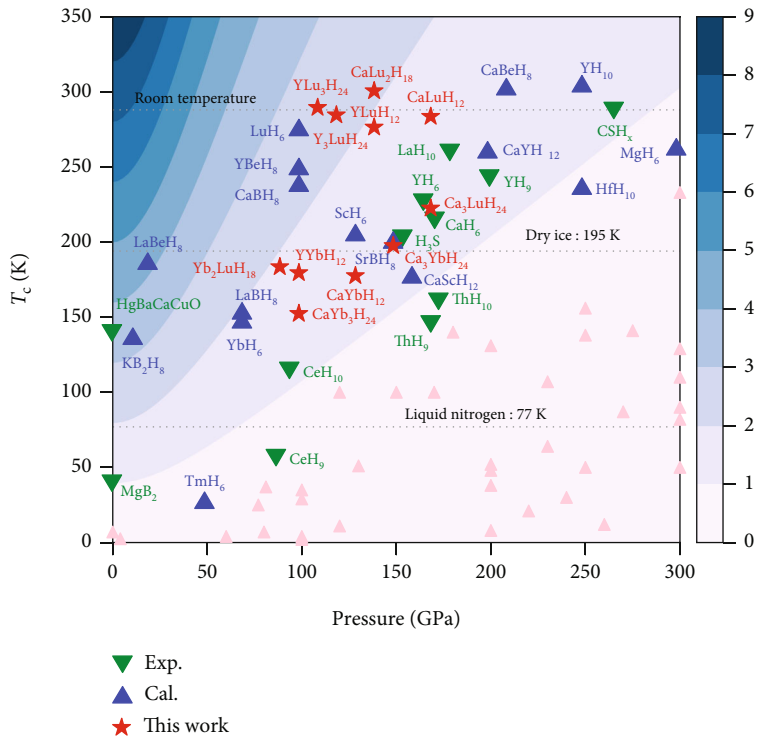

FIGURE 3: Pressure dependence of T_cs calculated for Yb/Lu substituted hexahydrides shown alongside other high-T_c superconductors. All thermodynamically stable hexahydrides and metastable phase $CaLu_2H_{18}$ in this work are marked with red stars. Blue triangles correspond to theoretical predictions [11, 17, 19, 20, 29, 32–34], green inverted triangles correspond to experimental measurements [1, 9, 14, 21, 22, 24, 26, 35–37], and pink triangles correspond to other less prominent results. The background is shaded according to the figure of merit S [38].

pressures of $Sc_{(1-x)}Yb_xH_6$ and $Yb_{(1-x)}Lu_xH_6$ decrease with the concentration of Yb doping (see Figures 2(f) and 2(g)). Especially $YbLuH_{12}$ and Yb_3LuH_{24}, which contain both heavy rare earth elements Yb and Lu, can be stable at 80 GPa and exhibit T_c of 198 K and 162 K, respectively. They have the lowest stable pressure in this work. To confirm the effect of 4f electrons on strengthening precompression, we calculated the phonon spectrum of $YbLuH_{12}$ at 80 GPa without considering the interactions of 4f electrons in valence electrons (see Figure S15). The calculated phonon spectrum exhibits imaginary frequencies in the whole Brillouin zone, indicating that $YbLuH_{12}$ is dynamically unstable. This result suggests that 4f electrons play an important role in stabilizing these clathrate structures.

The focus of hydrogen-based superconductor research is not simply the pursuit of high-temperature superconductivity, after the realization of room-temperature superconductivity. A good superconductor should achieve a good balance between the pressure required for stability and the critical temperature. Therefore, we use a figure of merit S [38] to evaluate the significance of all thermodynamically stable sodalite-like clathrate hexahydrides and metastable phase $CaLu_2H_{18}$ in this work. S is obtained from the critical temperature T_c and the pressure required for stabilization P:

$$S = \frac{T_c}{\sqrt{T_{c,MgB_2}^2 + P^2}}. \quad (1)$$

Y_3LuH_{24} and YLu_3H_{24} with $S > 2$ and $YLuH_{12}$ and Yb_2LuH_{18} with S close to 2 are better than the well-known hydrogen-based superconductor H_3S, LaH_{10}, and C-S-H compounds. Most importantly, it can be seen from Figure 3 that Y_3LuH_{24} is the room temperature superconductor with the lowest pressure required for stability (110 GPa), which is much lower than that of C-S-H, YH_{10} and $CaBeH_8$ with room-temperature superconducting. It also means that room-temperature superconductivity at moderate pressure is promising in hydrogen-based superconductors.

It seems difficult to summarize the law of T_c change only from the perspective of doping concentration for Lu-containing structures. So, we evaluated the distribution of H-H bond lengths for all hexahydrides in this work. Figure 4 shows the variation of superconducting critical temperature T_c and H-H bond lengths with the concentration of heavy rare earth element Lu/Yb in sodalite-like clathrate hexahydrides. There are nine hexahydrides with T_c over 250 K, including LuH_6, $YLuH_{12}$, YLu_3H_{24}, Y_3LuH_{24}, $CaLuH_{12}$, $CaLu_2H_{18}$, $CaLu_3H_{24}$, $ScLuH_{12}$, and $ScLu_3H_{24}$. They all have one thing in common, that is, the H-H bond lengths are all distributed around 1.25-1.30 Å (see Figures 4(a)–4(c)). The H-H bond length distribution may be an important factor on T_c for Lu-containing structures. The more H-H bond lengths are distributed around 1.25-1.30 Å, the higher T_c will be. Elongating the H-H bond length to more than 1.25 Å is an effective means to increase T_c. In the Yb-containing hexahydrides, Y_3YbH_{24}, Y_2YbH_{18},

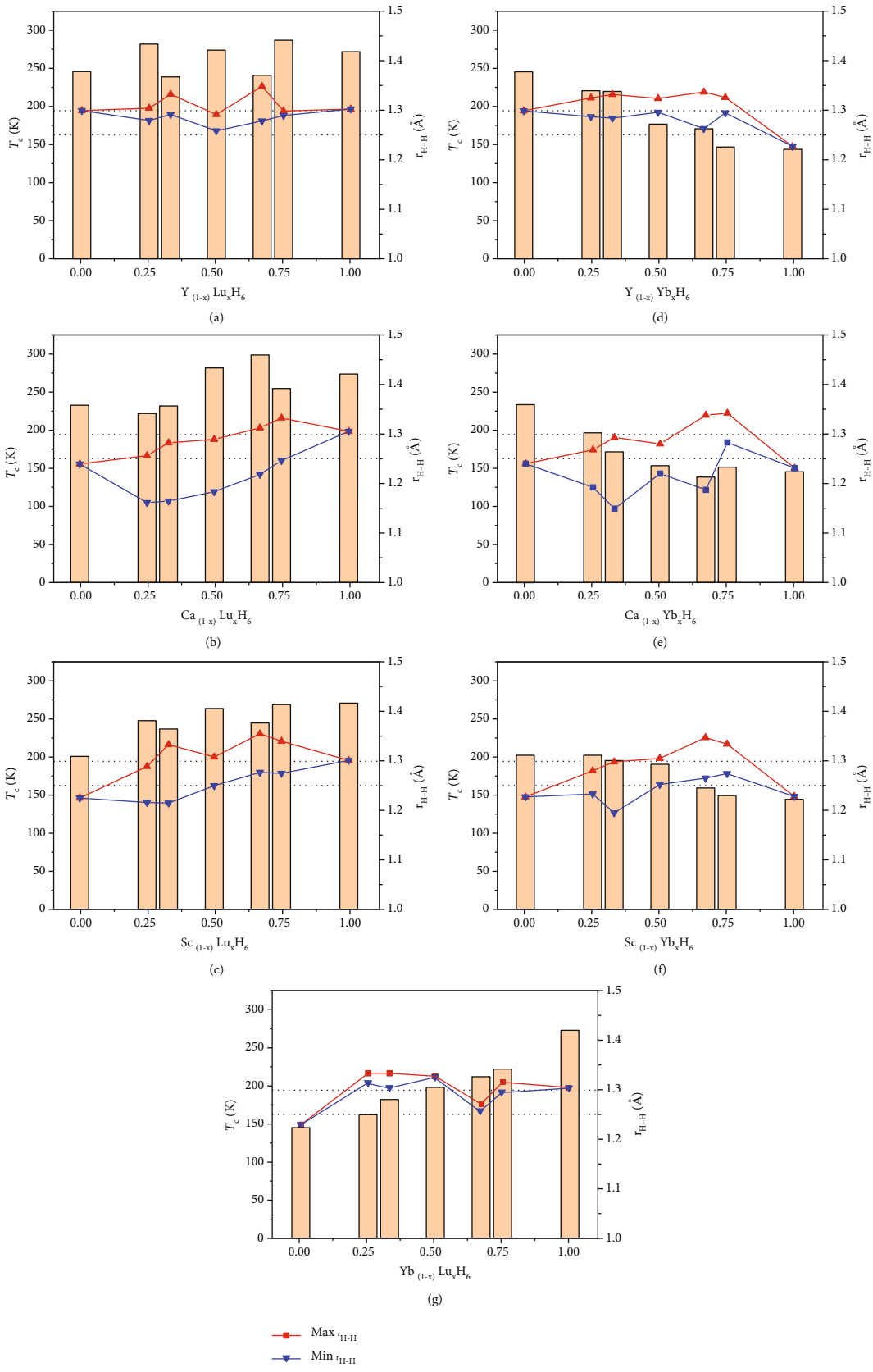

FIGURE 4: Maximum and minimum H-H bond lengths and calculated critical temperature T_cs as a function of doping concentration in (a) $Y_{(1-x)}Lu_xH_6$, (b) $Ca_{(1-x)}Lu_xH_6$, (c) $Sc_{(1-x)}Lu_xH_6$, (d) $Y_{(1-x)}Yb_xH_6$, (e) $Ca_{(1-x)}Yb_xH_6$, (f) $Sc_{(1-x)}Yb_xH_6$, and (g) $Yb_{(1-x)}Lu_xH_6$. Dashed lines correspond to bond lengths of 1.25 and 1.3 Å.

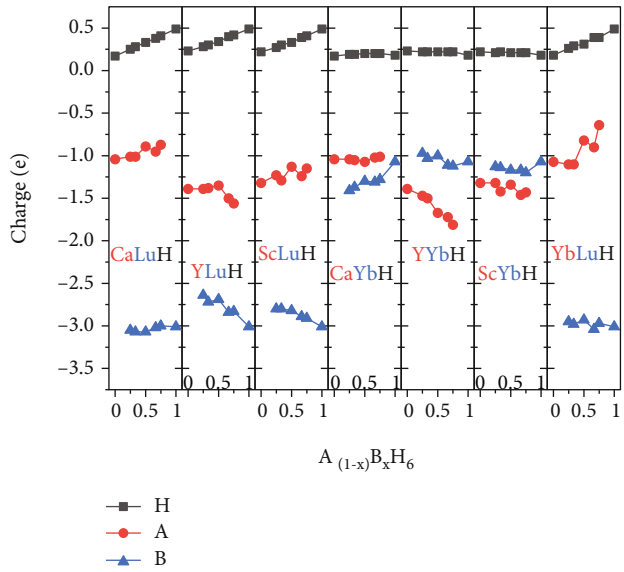

FIGURE 5: Charges transferred as a function of doping concentration between different elements in $A_{(1-x)}B_xH_6$. Negative means loss of electrons; positive means gain of electrons.

Sc_3YbH_{24}, $YbLu_2H_{18}$, and $YbLu_3H_{24}$ have T_c higher than 200 K, in which the H-H bond length distribution is also close to 1.25-1.30 Å (see Figures 4(d)–4(g)), compared to other Yb-containing hexahydrides. This means that the H-H bond length distribution is likely to be an important reference for finding high-temperature hydrogen-based superconductors in these sodalite-like clathrate hexahydrides.

Charge transfer is essential for the formation of hydrogen cages. The stability of H_{24} cages in clathrate hexahydrides comes from H_2 molecular units accepting electrons from the central metal atoms to form six H_4 units as the cornerstone of the construction of the three-dimensional sodalite gabion. Figure 5 shows the charge transfer between two "precompressor" metal elements and hydrogen in all sodalite-like clathrate hexahydrides we studied. It can be clearly seen that Lu element is an extremely good electron donor. Each Lu atom can donate 3.07 electrons at most, which is far more than other metal elements. The electrons obtained by H atom in the Lu-containing structures increase with increasing the Lu doping concentration (black curves). In the structures without Lu, the number of electrons obtained by H atom is basically the same level (about 0.23 $|e|$). Although Y atom is also ideal candidates for "precompressor" metal element, it can only donate up to 1.81 electrons. Ca, Sc, and Yb atoms cannot donate more than 1.5 electrons. Both YH_6 and CaH_6 exhibit high-temperature superconductivity, but they are still not qualified for room temperature superconductor. The introduction of Lu makes it possible to achieve room-temperature superconductivity in sodalite-like clathrate hexahydrides.

3. Discussion

According to the aforementioned findings, the critical temperatures of Y_3LuH_{24}, $YLuH_{12}$, and YLu_3H_{24} have reached room temperature under moderate pressure. In addition, although the T_c of Ca_3LuH_{24} is only 221 K at 170 GPa, it has a lower thermodynamically stable pressure (below 200 GPa), meaning that it is easier to be synthesized experimentally. To gain insight into the origin of room-temperature superconductivity for these sodalite-like clathrate hexahydrides, we calculated their electronic band structures and projected density of electronic states (PDOS), as shown in Figure 6. For hydrides, the contribution of electronic states of H to the Fermi level is an important basis for judging whether it is an excellent superconductor. In this work, for two structures of the same space group and the same "precompressor" metal elements A and B, their contributions of electronic states of H near the Fermi surface are basically the same. For example, the contributions of electronic states of H near the Fermi surface in YLu_3H_{24} and Y_3LuH_{24} are both 1.5 states/eV/f.u. (see Figures 6(a) and 6(b)), which is the essential reason for their close T_c.

In addition to H, f electrons also have an important impact on superconductivity and dynamical stability, especially in Yb-containing structures. Note that the 4f orbitals associated with the Yb atom form a set of localized bands that appear about 1.5 eV below the Fermi level (see Figures S19–S22). As the Yb doping concentration increases, the position of PDOS peak corresponding to the f electrons is always 1.5 eV below the Fermi level and does not shift, but the contribution of electronic states of the f electrons at the Fermi surface increases. The 4f-orbital electrons are good for stabilizing the structure, but excessive f electrons at the Fermi surface will negatively affect superconductivity. Therefore, the T_cs of Yb-containing structures in Table S1 mostly does not exceed 200 K. Although lowering the concentration of Yb can increase T_c, it also makes Yb lose its role in reducing the pressure required for stabilization. For Lu-containing structures, extra electron in the 5d orbitals leads to the 4f electrons moving away from the Fermi surface in the band structure (see Figures S19–S22). Thus, Lu-containing structures are not negatively affected by the 4f-orbital electrons, and exhibits a rather high T_c.

Meanwhile, YLu_3H_{24} can exhibit 288 K room temperature superconductivity which is also related to the flat band near the Fermi surface along the W-K direction, as shown in Figures 6(a) and 6(b). Such flat bands exist in all sodalite-like clathrate hexahydrides with Fm-3m space group in this work, but not all the flat bands can be near the Fermi surface. The energy bands of hydrides are influenced by the precompression element. Compared to CaH_6, YH_6 has a higher Fermi energy due to more valence electrons [19]. Ca_3LuH_{24} also has the same flat band, but at 1.7 eV above the Fermi energy (see Figure 6(d)). This results in that the contribution of electronic states of H in Ca_3LuH_{24} at the Fermi level is not as high as that in YLu_3H_{24}. It may be one of the reasons why the T_c of Ca_3LuH_{24} is not as high as that of YLu_3H_{24}. Due to the lower Lu content, the flat band of Y_3LuH_{24} is slightly above the Fermi surface compared to YLu_3H_{24} (see Figure 6(b)). Among all the "precompressor" metals, Y and Lu are more favorable for high-temperaturesuperconductivity of H_{24} cage. In ternary

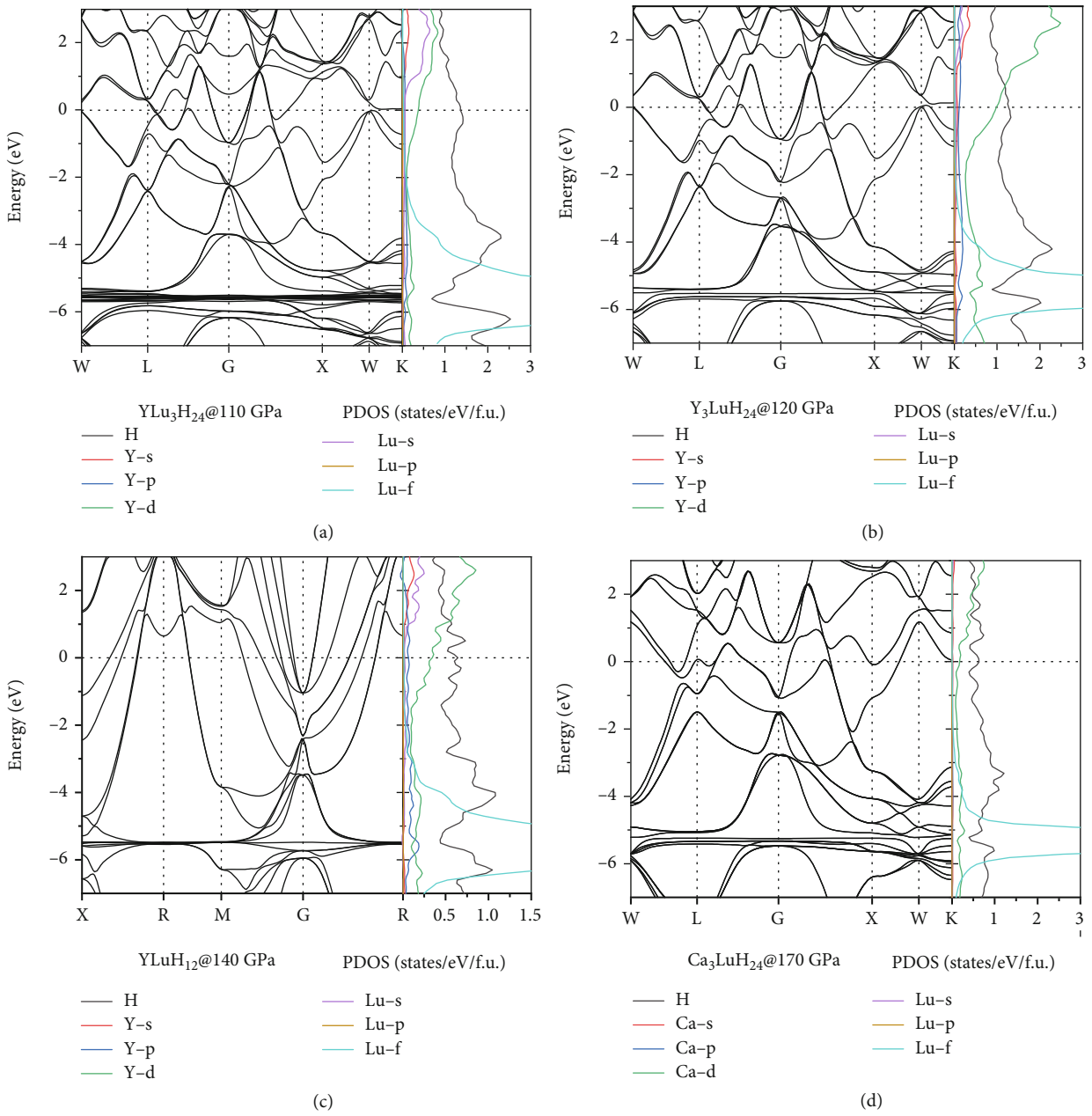

FIGURE 6: Electronic band structures and projected density of electronic states (PDOS) of (a) *Fm*-3m-YLu_3H_{24} at 110 GPa, (b) *Fm*-3*m*-Y_3LuH_{24} at 120 GPa, (c) *Pm*-3*m*-$YLuH_{12}$ at 140 GPa, and (d) *Fm*-3*m*-Ca_3LuH_{24} at 170 GPa.

clathrate hexahydrides $A_{1-x}B_xH_6$, by selecting the appropriate "precompressor" elements A and B, adjust their proportions, maximizing T_c can be achieved.

The high T_cs of hydrogen-based superconductors are largely due to strong electron-phonon coupling (EPC) from high frequency optical phonons. We calculated phonon spectrum, phonon density of state (PHDOS) and integral EPC parameter λ of all sodalite-like clathrate hexahydrides we studied, to explore the source of this strong coupling from optical phonons. As shown in Figure 7, the phonon spectra of these ternary clathrate structures are similar to those of the binary clathrate hexahydrides [15, 18]. The low frequency region is mainly the vibration of metal atoms (red and blue peak in PHDOS), and the high frequency region comes from the vibration of hydrogen (black peak in PHDOS). The maximum vibrational frequency of the hydrogen atom is related to the length of the H-H bond. The shorter the H-H bond, the higher the corresponding vibrational frequency. The maximum vibrational frequency of H_2 or H_3 units is generally above 2000 cm^{-1} [39]. The absence of spectral lines over 2000 cm^{-1} means that there are no H_2 or H_3 units. It can be seen from Figure 7 that the integral curve of λ (red curve) grows rapidly in 500-1500 cm^{-1}, while λ grows slowly above 1500 cm^{-1} (see Figure 7(d)). It means that the vibration in frequency range of 500-1500 cm^{-1} is the most important source of electron-

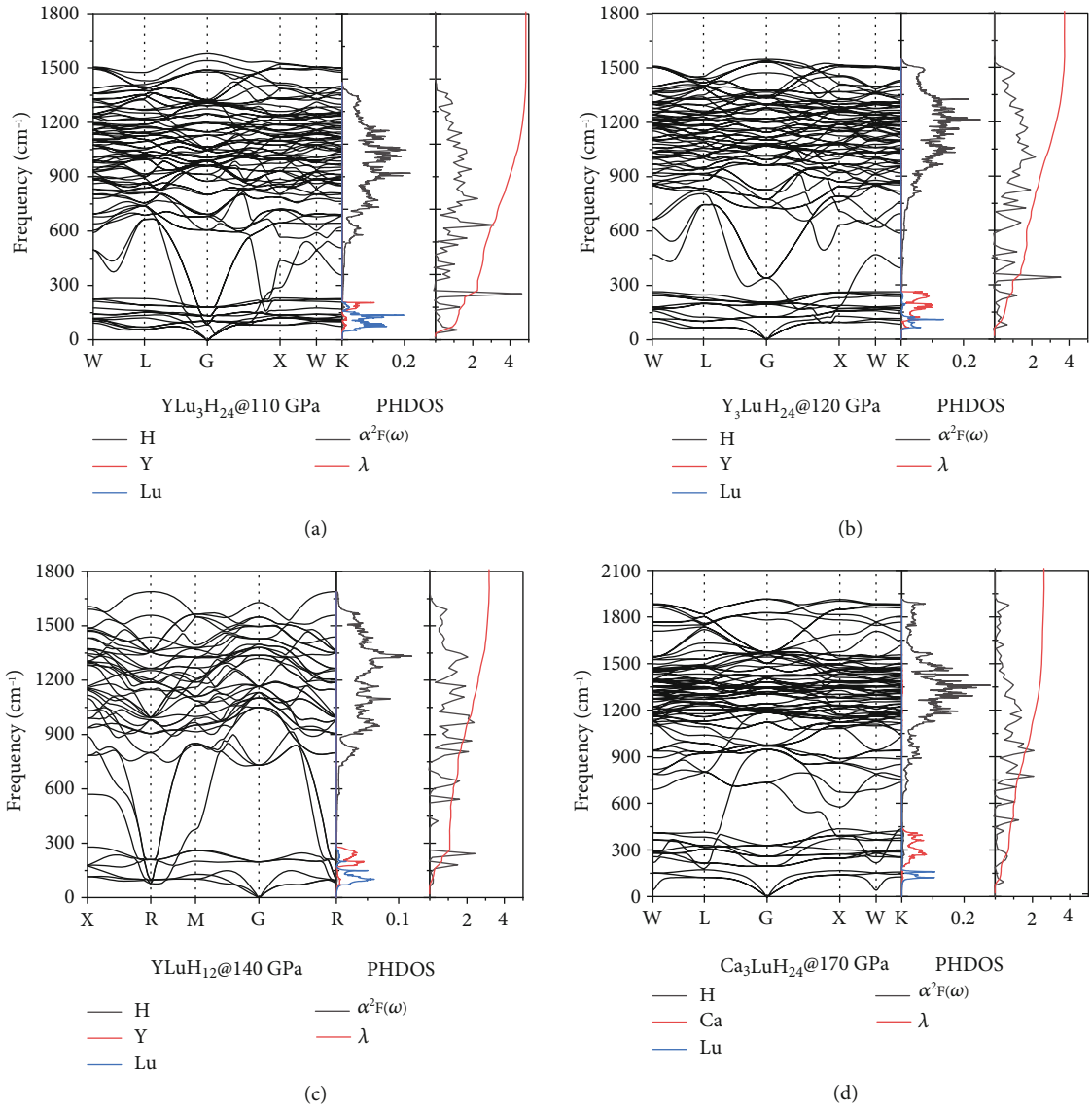

FIGURE 7: Phonon dispersion, phonon density of state (PHDOS), spectral function $\alpha^2F(\omega)$ and integral EPC parameter λ of (a) *Fm*-3m-YLu_3H_{24} at 110 GPa, (b) *Fm*-3*m*-Y_3LuH_{24} at 120 GPa, (c) *Pm*-3*m*-$YLuH_{12}$ at 140 GPa, and (d) *Fm*-3*m*-Ca_3LuH_{24} at 170 GPa.

phonon coupling. By comparing the phonon spectrum (see Figures S9–S15) and bond length (see Figure 4) of all sodalite-like clathrate hexahydrides, we find that the H-H bond length corresponding to this vibrational frequency range is about 1.25-1.30 Å, which is consistent with the most suitable H-H bond length summarized in Figure 4. Elongating the H-H bond to 1.25-1.30 Å can reduce the vibrational frequency of hydrogen from high frequency (above 1500 cm^{-1}) to a suitable frequency of 500-1500 cm^{-1}, thereby increasing T_c.

In addition to the high frequency optical phonons, "soft mode" also plays an important role in enhancement of superconductivity [40, 41]. It can be seen from YLu_3H_{24} (Figure 7(a)) that there are some soft phonon modes near the Gamma point in frequency range of 100-500 cm^{-1}. The integral curve of λ (red curve) grows rapidly in this frequency range which can reach 3 up to 500 cm^{-1}. The Y_3LuH_{24} and $YLuH_{12}$ also have soft phonon modes (see Figures 7(b) and 7(c)). The integral curve of λ corresponding to the frequency at which the phonon softening is also rising rapidly. These results indicate that in YLu_3H_{24}, Y_3LuH_{24}, and $YLuH_{12}$ near lattice instability, the phonon softening strengthens the electron-phonon coupling λ, which in turn leads to high T_c.

In conclusion, the incorporation of heavy rare earth elements Yb/Lu is an effective method to tune the superconducting transition temperature and the required pressure for stabilization of sodalite-like clathrate hydrides. In particular, the introduction of Lu element can further improve the superconductivity and keep the low-pressure stability. The three most prominent compounds Y_3LuH_{24} (283 K at 120 GPa), $YLuH_{12}$ (275 K 140 GPa), and YLu_3H_{24} (288 K at 110 GPa) exhibit room temperature superconductivity at much lower pressure than that of previously discovered

room temperature superconductors, such as C-S-H, YH_{10}, and $CaBeH_8$. The enhancement of T_c is achieved by adjusting the H-H bond length to affect the hydrogen vibrational frequency and thereby enhance the electron-phonon coupling. Our results represent an important step towards room-temperature superconductivity at ambient pressure and will stimulate further experimental exploration.

4. Computational Methods

High-pressure structure searches were performed using the *ab initio* random structure searching (AIRSS) technique [42, 43]. For Ca-Lu-H, Y-Lu-H, and Yb-Lu-H systems, we predicted more than 8000 structures using variable composition structure searches in each system for their ternary convex hulls. Furthermore, for 36 $A_{1-x}B_xH_6$ (A = Ca, Y, Sc, B=Yb, Lu, and A = Yb, B = Lu, x = 0.25, 0.33, 0.5, 0.67, 0.75), we predicted about 500 structures for each composition. Structure relaxations during structure searches were performed using the *ab initio* calculation of the Cambridge Serial Total Energy Package (CASTEP) code [44]. The generalized gradient approximation with the Perdew-Burke-Ernzerhof parametrization [45] for the exchange-correlation functional and ultrasoft pseudopotentials with cut-off energy of 400 eV and Brillouin zone sampling grid spacing of $2\pi \times 0.07$ Å^{-1} were chosen for the structure searching.

Considering the results of pseudopotential detection for Yb-H and Lu-H in previous work [20], we used CASTEP with ultrasoft pseudopotentials for structural relaxation and calculations of enthalpies and electronic properties. A cut-off energy of 1000 eV and a Brillouin zone sampling grid spacing of $2\pi \times 0.03$ Å^{-1} were used. All enthalpy calculations are well converged to less than 1 meV per atom, which is acceptable for density functional theoretical calculations. The charge transfer calculations are obtained using Mulliken population analysis [46].

The Quantum-ESPRESSO package [47] was used in phonon and electron−phonon calculations. Ultrasoft pseudopotentials were used with a kinetic energy cut-off of 90 Ry. The k-point and q-point meshes in the first Brillouin zone of $12 \times 12 \times 12$ and $4 \times 4 \times 4$ grids were adopted, respectively. The superconductive transition temperatures are estimated through the Allen−Dynes-modified McMillan equation (A-D-M) [48] with correction factors and self-consistent solution of the Eliashberg equation (scE) [49] with the Coulomb pseudopotential $\mu^* = 0.10$ and 0.13.

Data Availability

The data supporting the findings of this study are available within the article and its Supplementary Materials files and from the corresponding author upon reasonable request.

Disclosure

This paper is dedicated to the 70th anniversary of the physics of Jilin University. Parts of calculations were performed in the High Performance Computing Center (HPCC) of Jilin University and TianHe-1 (A) at the National Supercomputer Center in Tianjin.

Conflicts of Interest

The authors declare that there is no conflict of interest regarding the publication of this article.

Authors' Contributions

Defang Duan and Tian Cui initiated the project. Mingyang Du performed the most of the theoretical calculations and contributed to the data interpretation and writing the manuscript. Zihan Zhang and Hao Song contributed to the theoretical calculations. All authors contributed to the discussion and the final version of the manuscript.

Acknowledgments

This work was supported by National Natural Science Foundation of China (grant nos. 12122405, 52072188, and 51632002), National Key R&D Program of China (no. 2018YFA0305900), Program for Changjiang Scholars and Innovative Research Team in University (no. IRT_15R23), and Jilin Provincial Science and Technology Development Project (20210509038RQ).

Supplementary Materials

Supplementary information is available and includes convex hull, phonon spectrum, band structures, superconductivity properties, and lattice parameters. *(Supplementary Materials)*

References

[1] A. Schilling, M. Cantoni, J. D. Guo, and H. R. Ott, "Superconductivity above 130 K in the Hg-Ba-Ca-Cu-O system," *Nature*, vol. 363, no. 6424, pp. 56–58, 1993.

[2] L. Gao, Y. Y. Xue, F. Chen et al., "Superconductivity up to 164 k in $HgBa_2Ca_mCu_mO_{2m+2+\delta}$ (m=1, 2, and 3) under quasihydrostatic pressures," *Physical Review B*, vol. 50, no. 6, pp. 4260–4263, 1994.

[3] T. Liu, C. He, F. Wang et al., "Shockwave-loading-induced enhancement of Tc in superconducting $Bi_2Sr_2CaCu_2O_{8+\delta}$," *Scientific Reports*, vol. 7, no. 1, p. 6710, 2017.

[4] M. Du, W. Zhao, T. Cui, and D. Duan, "Compressed superhydrides: the road to room temperature superconductivity," *Journal of Physics: Condensed Matter*, vol. 34, article 173001, 2022.

[5] D. F. Duan, Y. X. Liu, Y. B. Ma, Z. Shao, B. Liu, and T. Cui, "Structure and superconductivity of hydrides at high pressures," *National Science Review*, vol. 4, no. 1, pp. 121–135, 2017.

[6] L. P. Gor'kov and V. Z. Kresin, "Colloquium: high pressure and road to room temperature superconductivity," *Reviews of Modern Physics*, vol. 90, no. 1, p. 16, 2018.

[7] D. Duan, Y. Liu, F. Tian et al., "Pressure-induced metallization of dense $(H_2S)_2H_2$ with high-Tc superconductivity," *Scientific Reports*, vol. 4, p. 6, 2015.

[8] D. F. Duan, X. L. Huang, F. B. Tian et al., "Pressure-induced decomposition of solid hydrogen sulfide," *Physical Review B*, vol. 91, no. 18, p. 5, 2015.

[9] A. P. Drozdov, M. I. Eremets, I. A. Troyan, V. Ksenofontov, and S. I. Shylin, "Conventional superconductivity at 203 kelvin at high pressures in the sulfur hydride system," *Nature*, vol. 525, no. 7567, pp. 73–76, 2015.

[10] M. Einaga, M. Sakata, T. Ishikawa et al., "Crystal structure of the superconducting phase of sulfur hydride," *Nature Physics*, vol. 12, no. 9, pp. 835–838, 2016.

[11] H. Y. Liu, I. I. Naumov, R. Hoffmann, N. W. Ashcroft, and R. J. Hemley, "Potential high-Tc superconducting lanthanum and yttrium hydrides at high pressure," *Proceedings of the National Academy of Sciences of the United States of America*, vol. 114, no. 27, pp. 6990–6995, 2017.

[12] F. Peng, Y. Sun, C. J. Pickard, R. J. Needs, Q. Wu, and Y. Ma, "Hydrogen clathrate structures in rare earth hydrides at high pressures: possible route to room-temperature superconductivity," *Physical Review Letters*, vol. 119, no. 10, p. 6, 2017.

[13] A. P. Drozdov, P. P. Kong, V. S. Minkov et al., "Superconductivity at 250 K in lanthanum hydride under high pressures," *Nature*, vol. 569, no. 7757, pp. 528–531, 2019.

[14] M. Somayazulu, M. Ahart, A. K. Mishra et al., "Evidence for superconductivity above 260 K in lanthanum superhydride at megabar pressures," *Physical Review Letters*, vol. 122, no. 2, 2019.

[15] H. Wang, J. S. Tse, K. Tanaka, T. Iitaka, and Y. Ma, "Superconductive sodalite-like clathrate calcium hydride at high pressures," *Proceedings of the National Academy of Sciences of the United States of America*, vol. 109, no. 17, pp. 6463–6466, 2012.

[16] M. Gubler, J. A. Flores-Livas, A. Kozhevnikov, and S. Goedecker, "Missing theoretical evidence for conventional room-temperature superconductivity in low-enthalpy structures of carbonaceous sulfur hydrides," *Physical Review Materials*, vol. 6, no. 1, article 014801, 2022.

[17] X. Feng, J. Zhang, G. Gao, H. Liu, and H. Wang, "Compressed sodalite-like MgH_6 as a potential high-temperature superconductor," *RSC Advances*, vol. 5, no. 73, pp. 59292–59296, 2015.

[18] Y. Li, J. Hao, H. Liu, J. S. Tse, Y. Wang, and Y. Ma, "Pressure-stabilized superconductive yttrium hydrides," *Scientific Reports*, vol. 5, no. 1, p. 9948, 2015.

[19] K. Abe, "Hydrogen-rich scandium compounds at high pressures," *Physical Review B*, vol. 96, no. 14, p. 144108, 2017.

[20] H. Song, Z. Zhang, T. Cui, C. J. Pickard, V. Z. Kresin, and D. Duan, "High Tc superconductivity in heavy rare earth hydrides," *Chinese Physics Letters*, vol. 38, no. 10, p. 107401, 2021.

[21] L. Ma, K. Wang, Y. Xie et al., "High-temperature superconducting phase in clathrate calcium hydride CaH_6 up to 215 K at a pressure of 172 GPa," *Physical Review Letters*, vol. 128, no. 16, p. 167001, 2022.

[22] I. A. Troyan, D. V. Semenok, A. G. Kvashnin et al., "Anomalous high-temperature superconductivity in YH_6," *Advanced Materials*, vol. 33, no. 15, article 2006832, 2021.

[23] S. Yao, C. Wang, S. Liu, H. Jeon, and J. H. Cho, "Formation mechanism of chemically precompressed hydrogen clathrates in metal superhydrides," *Inorganic Chemistry*, vol. 60, no. 17, pp. 12934–12940, 2021.

[24] W. Chen, D. V. Semenok, X. Huang et al., "High-temperature superconducting phases in cerium superhydride with a Tc up to 115 K below a pressure of 1 megabar," *Physical Review Letters*, vol. 127, no. 11, article 117001, 2021.

[25] Y. Sun, J. Lv, Y. Xie, H. Liu, and Y. Ma, "Route to a superconducting phase above room temperature in electron-doped hydride compounds under high pressure," *Physical Review Letters*, vol. 123, no. 9, p. 5, 2019.

[26] E. Snider, N. Dasenbrock-Gammon, R. McBride et al., "Room-temperature superconductivity in a carbonaceous sulfur hydride," *Nature*, vol. 586, no. 7829, pp. 373–377, 2020.

[27] T. Wang, M. Hirayama, T. Nomoto, T. Koretsune, R. Arita, and J. A. Flores-Livas, "Absence of conventional room-temperature superconductivity at high pressure in carbon-doped H_3S," *Physical Review B*, vol. 104, no. 6, article 064510, 2021.

[28] M. Du, Z. Zhang, T. Cui, and D. Duan, "Pressure-induced superconducting CS_2H_{10} with an H_3S framework," *Physical Chemistry Chemical Physics*, vol. 23, no. 39, pp. 22779–22784, 2021.

[29] Z. Zhang, T. Cui, M. J. Hutcheon et al., "Design principles for high-temperature superconductors with a hydrogen-based alloy backbone at moderate pressure," *Physical Review Letters*, vol. 128, no. 4, article 047001, 2022.

[30] D. V. Semenok, I. A. Troyan, A. G. Ivanova et al., "Superconductivity at 253 K in lanthanum–yttrium ternary hydrides," *Materials Today*, vol. 48, pp. 18–28, 2021.

[31] L. Deng, T. Bontke, R. Dahal et al., "Pressure-induced high-temperature superconductivity retained without pressure in fese single crystals," *Proceedings of the National Academy of Sciences of the United States of America*, vol. 118, no. 28, 2021.

[32] M. Gao, X.-W. Yan, Z.-Y. Lu, and T. Xiang, "Phonon-mediated high-temperature superconductivity in the ternary borohydride KB_2H_8 under pressure near 12 GPa," *Physical Review B*, vol. 104, no. 10, article L100504, 2021.

[33] H. Xie, D. F. Duan, Z. J. Shao et al., "High-temperature superconductivity in ternary clathrate $YCaH_{12}$ under high pressures," *Journal of Physics: Condensed Matter*, vol. 31, no. 24, article 245404, 2019.

[34] H. Xie, Y. Yao, X. Feng et al., "Hydrogen pentagraphenelike structure stabilized by hafnium: a high-temperature conventional superconductor," *Physical Review Letters*, vol. 125, no. 21, article 217001, 2020.

[35] P. Kong, V. S. Minkov, M. A. Kuzovnikov et al., "Superconductivity up to 243 K in the yttrium-hydrogen system under high pressure," *Nature Communications*, vol. 12, no. 1, p. 5075, 2021.

[36] D. V. Semenok, A. G. Kvashnin, A. G. Ivanova et al., "Superconductivity at 161 k in thorium hydride ThH_{10}, synthesis and properties," *Materials Today*, vol. 33, pp. 36–44, 2020.

[37] J. Nagamatsu, N. Nakagawa, T. Muranaka, Y. Zenitani, and J. Akimitsu, "Superconductivity at 39 K in magnesium diboride," *Nature*, vol. 410, no. 6824, pp. 63-64, 2001.

[38] C. J. Pickard, I. Errea, and M. I. Eremets, "Superconducting hydrides under pressure," *Annual Review of Condensed Matter Physics*, vol. 11, no. 1, pp. 57–76, 2020.

[39] M. Du, Z. Zhang, H. Song et al., "High-temperature superconductivity in transition metallic hydrides MoH_{11} (Mo, W, Nb, and Ta) under high pressure," *Physical Chemistry Chemical Physics*, vol. 23, no. 11, pp. 6717–6724, 2021.

[40] X.-J. Chen, "Exploring high-temperature superconductivity in hard matter close to structural instability," *Matter and Radiation at Extremes*, vol. 5, no. 6, article 068102, 2020.

[41] Y. Quan, S. S. Ghosh, and W. E. Pickett, "Compressed hydrides as metallic hydrogen superconductors," *Physical Review B*, vol. 100, no. 18, article 184505, 2019.

[42] C. J. Pickard and R. J. Needs, "High-pressure phases of silane," *Physical Review Letters*, vol. 97, p. 4, 2006.

[43] C. J. Pickard and R. J. Needs, "Ab initiorandom structure searching," *Journal of Physics: Condensed Matter*, vol. 23, no. 5, article 053201, 2011.

[44] S. J. Clark, M. D. Segall, C. J. Pickard et al., "First principles methods using castep," *Zeitschrift Für Kristallographie-Crystalline Materials*, vol. 220, no. 5-6, pp. 567–570, 2005.

[45] J. P. Perdew, K. Burke, and M. Ernzerhof, "Generalized gradient approximation made simple," *Physical Review Letters*, vol. 77, no. 18, pp. 3865–3868, 1996.

[46] M. D. Segall, R. Shah, C. J. Pickard, and M. C. Payne, "Population analysis of plane-wave electronic structure calculations of bulk materials," *Physical Review B*, vol. 54, no. 23, pp. 16317–16320, 1996.

[47] P. Giannozzi, S. Baroni, N. Bonini et al., "Quantum espresso: a modular and open-source software project for quantum simulations of materials," *Journal of Physics: Condensed Matter*, vol. 21, p. 19, 2009.

[48] P. B. Allen and R. C. Dynes, "Transition temperature of strong-coupled superconductors reanalyzed," *Physical Review B*, vol. 12, no. 3, pp. 905–922, 1975.

[49] G. M. Eliashberg, "Interactions between electrons and lattice vibrations in a superconductor," *Soviet Physics, Journal of Experimental and Theoretical Physics*, vol. 11, no. 3, pp. 696–702, 1960.